



ELSEVIER

Available online at [www.sciencedirect.com](http://www.sciencedirect.com)

SCIENCE @ DIRECT®

Nuclear Instruments and Methods in Physics Research A 535 (2004) 25–35

NUCLEAR  
INSTRUMENTS  
& METHODS  
IN PHYSICS  
RESEARCH  
Section A

[www.elsevier.com/locate/nima](http://www.elsevier.com/locate/nima)

# High-energy physics experiments in space

Franco Cervelli

*Istituto Nazionale di Fisica Nucleare (INFN), via Vecchiali Vornese 1291, Pisa 56010, Italy*

Available online 19 August 2004

---

## Abstract

The main environmental difficulties related to HEP experimentation on satellites and balloons are described. We review ways how to face these difficulties, analyzing some paradigmatic examples of present and future experiments.

Furthermore, the main features of detectors operating outside the terrestrial atmosphere are reported, concentrating in particular on energy and momentum measurements and on particle identification.

© 2004 Elsevier B.V. All rights reserved.

*PACS:* 07.87.+v; 95.55.–h

*Keywords:* Cosmic rays; Satellite experiment; Space born experiment

---

## 1. Introduction

At present a new synthesis is taking place in Physics, i.e. that of Cosmology and Particle Physics. In fact, there are many relevant “common” questions between Astrophysics and Sub-nuclear Physics, such as:

- (a) Where are cosmic rays (CR) accelerated? Which are the mechanisms of such an acceleration?
- (b) Can we understand the particle interactions at very high energies?
- (c) Do particles exist in CR which have not yet been observed with modern accelerators?
- (d) What is the chemical composition of CR?

To answer these questions, CR are studied with a large variety of detectors (see Fig. 1). Whether CR are studied in underground detectors or observed in outer space, modern Astrophysics makes always use of the technologies of Subnuclear Physics. Due to the primary interactions of CR with the atmosphere, large fluxes of  $\pi$ ,  $\mu$ ,  $p$ ,  $\bar{p}$  etc. are produced and their relative abundances are hard to predict. So the efficient identification of primary CRs is difficult.

A more “friendly” environment to do this kind of measurements is space, where CR can be directly detected. When studying CR in space, acceptance and exposure time are the figures of merit: their product determines the statistics of the measurements and, consequently, the accuracy of the observations. These factors also give rise to the difference between measurements performed on

---

*E-mail address:* [franco.cervelli@pi.infn.it](mailto:franco.cervelli@pi.infn.it) (F. Cervelli).

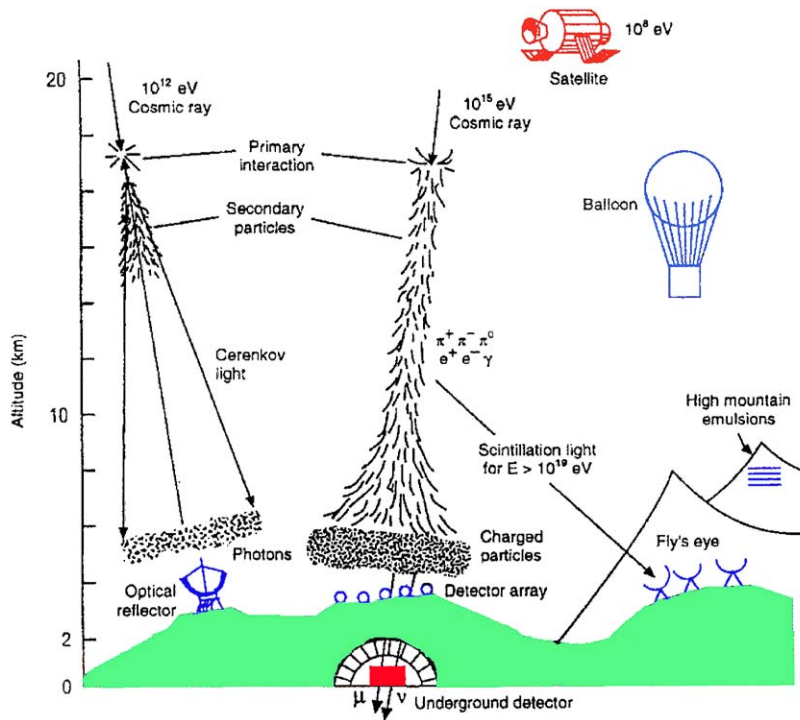


Fig. 1. Schematic view of present detectors studying CRs.

balloons and on satellites. While in space CR can be observed directly, it must also be said that some environmental difficulties have to be faced:

- strong mechanical stresses at launch and landing
- high variations in temperature
- absence of atmosphere (vacuum)
- limited electric power sources; no reference ground.

To explain the consequences of these peculiarities when projecting and operating particle detectors in space, we will mostly use the following four experiments as examples: Pamela [1], Glast [2], AMS-02 [3] and Euso [4].

## 2. Environmental difficulties

### 2.1. Mechanical stresses

At the moment of the carrier's launch or landing, experimental apparatuses must be able

to withstand accelerations of up to 20g (crash landing) and to damp vibrations over a wide range of frequencies and amplitudes. To satisfy these mechanical requirements, refined Finite Element Analyses are needed during the design phase (see Fig. 2), and construction materials must be carefully selected. Furthermore, careful experimental vibration tests [5] have to be performed (a) to check the structural capability to support stresses and (b) to measure the fundamental vibration frequencies of any relevant part of the detector in order to avoid dangerous resonances (see Fig. 3).

### 2.2. Temperature

During flight, in the external parts of the detectors the temperature varies from  $-40$  up to  $+40^\circ\text{C}$ . As a consequence, refined thermal detection is necessary to monitor at any time heating or freezing processes.

Furthermore, for a proper management of thermal sources the heat produced by the detector components must also be taken into account and

MSC.Patran 2000 r2 26-Feb-02 17:24:34

Fringe: SC1: ANALISI MODALE VINCOLATA, A1:Mode 2 : Freq. = 75.366: Eigenvectors, Translational-(NON-LAYERED) (MAG)

Deform: SC1: ANALISI MODALE VINCOLATA, A1:Mode 2 : Freq. = 75.366: Eigenvectors, Translational-(NON-LAYERED) (MAG)

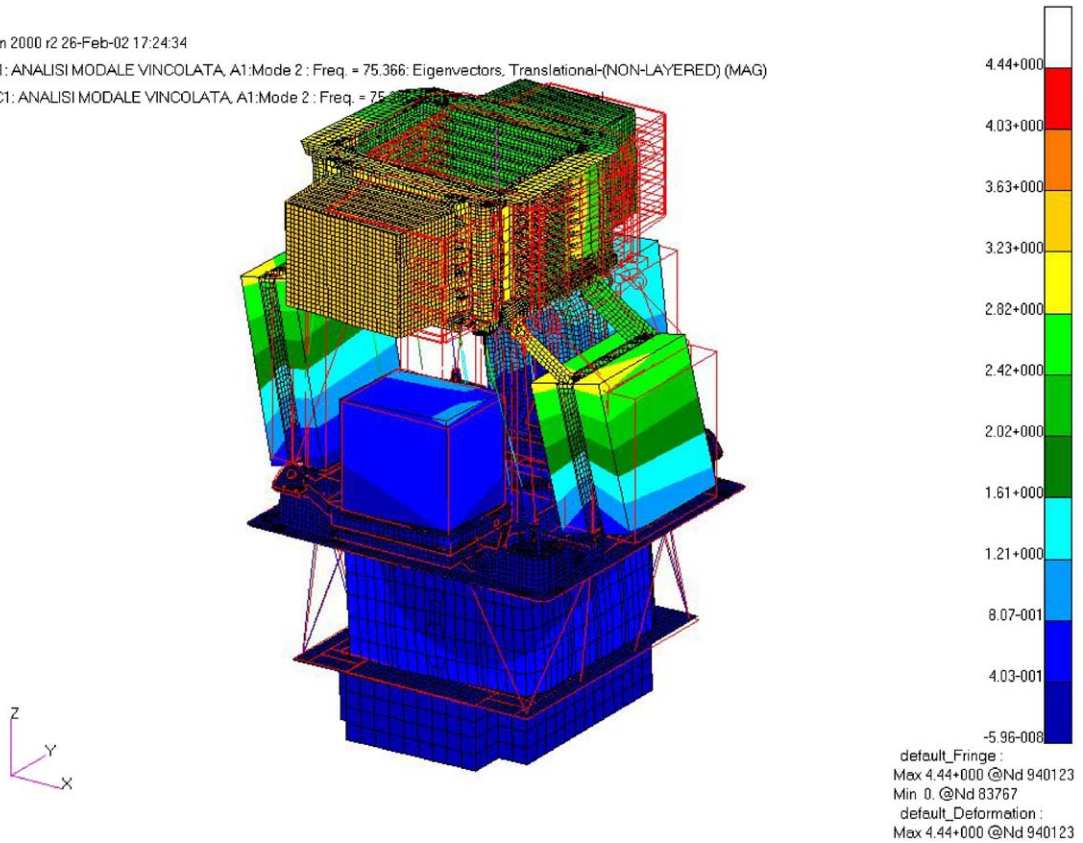


Fig. 2. Result of Finite Element Analyses for the Pamela Experiment.

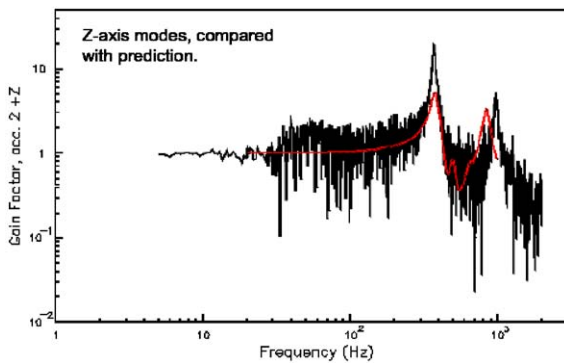


Fig. 3. Vibration tests to check the mechanical stability of the Glast Tracking Detectors: the two peaks correspond to the first and second eigenfrequency, respectively, for vibrations along the vertical axis.

one must pay attention to the fact that heat can be dissipated only by radiation. Also concerning thermal stresses, accurate studies are required at the project level (see Fig. 4); thermal tests (reproducing the temperature changes along orbits) are needed as well to verify the correct operation of the electronics, check for possible expansion or contraction of materials, etc. The use of gas detectors also requires dedicated measures: e.g., to use a MWPC with TMAE, condensation of this additive on the internal walls must be prevented to avoid discharges.

### 2.3. Electric power

To power detectors in space, two different strategies are followed. On balloons, lithium

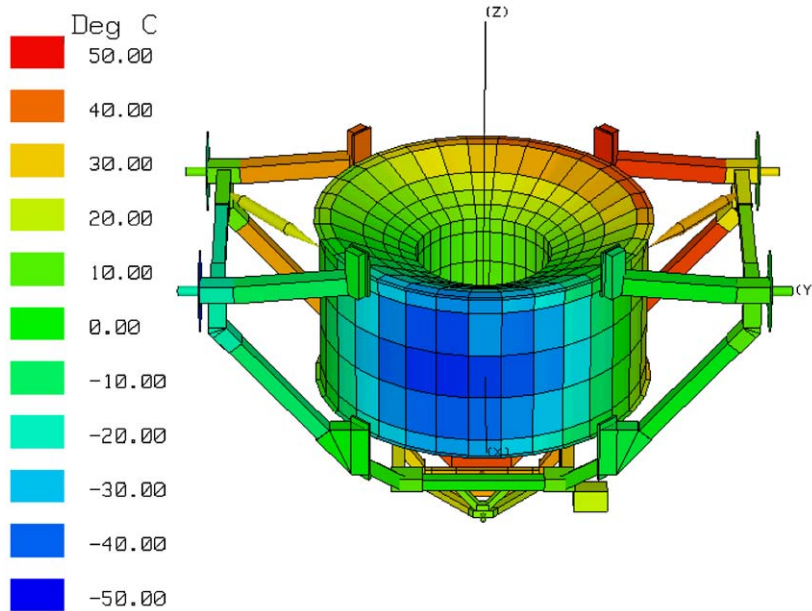


Fig. 4. Study of the thermal gradients for the AMS Experiment.

batteries are commonly used, providing  $\sim 50$  Ah for 300 g of weight. As a consequence, the experiment's weight budget depends strongly on the requirements concerning electric power: the BESS experiment [6], for example, had to increase its payload by 200 kg to produce the required 1.2 kW of power.

On satellites the standard source of electric power are solar panels, which have negligible weight and provide  $\sim 10$  W/m<sup>2</sup>.

### 3. Particle detectors in space

The design of a space-based particle detector must satisfy not only the physics targets but also the requirements imposed by the surrounding environment. In particular the main constraints stem from

- (a) dimensions
- (b) weight
- (c) mechanical stability
- (d) limited use of glue for mechanical assembly
- (e) low electric power
- (f) ground loops.

#### 3.1. Momentum measurements: magnets

The momentum resolution of any magnetic spectrometer is determined by the relation

$$\frac{\delta p}{p} = \sqrt{\left(k \frac{\sigma_0}{BL^2} p\right)^2 + \left(h \frac{\sqrt{x}}{\beta BL}\right)^2}$$

where  $k$  is a constant depending on the resolution and on the geometrical disposition of the tracking device,  $h$  is another constant depending on tracking material,  $\sigma_0$  is the accuracy on coordinates measurements,  $x$  is the thickness of the tracker (in radiation lengths), while  $L$  and  $B$  are the path of the particle in the magnetic field and the magnetic field strength, respectively.

To increase the momentum resolution, the product  $BL^2$  has to be maximized, but in space this also means larger dimensions and larger weights.

In practice, strong  $B$  fields are created either by permanent magnets or by superconducting magnets. At present strong  $B$  fields are made possible by the development of Nd–B–Fe alloys. For these magnets the residual induction (IR) is very close to the theoretical limit (14.5 kG vs. 16 kG), and  $B$

may be maximized according to:

$$B = IR \frac{R_0 - R_i}{R_i},$$

where  $R_0$  and  $R_i$  are a cylinder’s external and internal radius, respectively. So, for permanent magnets one tends to choose a short magnet with large  $R_0$  as far as compatible with a uniform  $B$

field. Typically, permanent magnets can provide:  $B \sim 1.5\text{--}4\text{ kG}$ , thus ensuring a Maximum Detectable Rigidity (MDR) of the order of  $\sim 500\text{ GeV/e}$ , for tracking resolutions of  $\sim 5\mu$  over a 1 m long magnetic field.

In space the use of superconducting magnets is favored by the limited power requirements, so that stronger fields can be easily reached

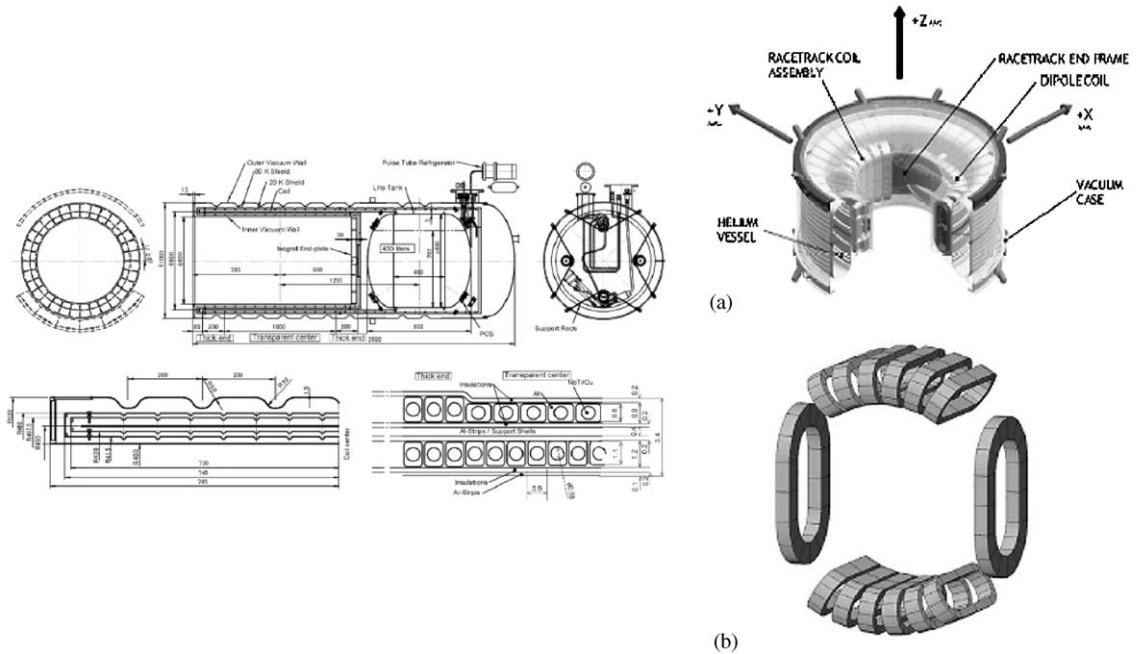


Fig. 5. Two examples of Superconducting magnets for HEP experiment in space: BESS (Solenoid) and AMS-02 (dipole).

Table 1  
Design parameters for the superconducting magnets of AMS-02 and BESS-Polar

	EGRET	AGILE
Mass	1830 kg	65 kg
Energy band	30 MeV–30 GeV	30 MeV–50 GeV
Field of view	$\sim 0.5\text{ sr}$	$\sim 3\text{ sr}$
PSF (67% containment radius)	$5.5^\circ$	$4.7^\circ$ (@ 0.1 GeV)
	$1.3^\circ$	$0.6^\circ$ (@ 1 GeV)
	$0.5^\circ$	$0.2^\circ$ (@ 10 GeV)
Dead time for $\gamma$ -ray detection	$\geq 100\text{ ms}$	$\leq 100\text{ }\mu\text{s}$
Sensitivity	$8 \times 10^{-9}$	$6 \times 10^{-9}$ (@ 0.1 GeV)
for point-like sources†	$1 \times 10^{-10}$	$4 \times 10^{-11}$ (@ 1 GeV)
( $\text{ph cm}^{-2}\text{ s}^{-1}\text{ MeV}^{-1}$ )	$1 \times 10^{-11}$	$3 \times 10^{-12}$ (@ 10 GeV)
Required pointing reconstruction	$\sim 10\text{ arcmin}$	$\sim 1\text{ arcmin}$

(a factor of  $\sim 10$  can be gained with respect to permanent magnets). Superconducting magnets are lighter in comparison and guarantee



Fig. 6. View of the Pamela magnetic spectrometer prototype.

uniform fields. However, these magnets suffer thermal day–night variations (and therefore need very good insulation), they need a liquid reserve (thus limiting the experiment’s life–time) and also require a stiff mechanical structure. Fig. 5 shows the structure of two different magnets, a solenoid (BESS) and a dipole (AMS-02): their design parameters are reported in Table 1.

### 3.2. Tracking systems

Silicon tracking represents a solution perfectly suitable for spectrometric analysis in space. The choice of small (Fig. 6) or large (Fig. 7) tracking devices is only determined by the available weight budget and standard resolutions are usually obtained (Fig. 8).

### 3.3. Particle identification

When the particle momentum ( $p$ ) and velocity ( $\beta$ ) are known, the particle mass ( $m$ ) is obtained by

$$m = ZeR \sqrt{\frac{1}{\beta^2} - 1},$$

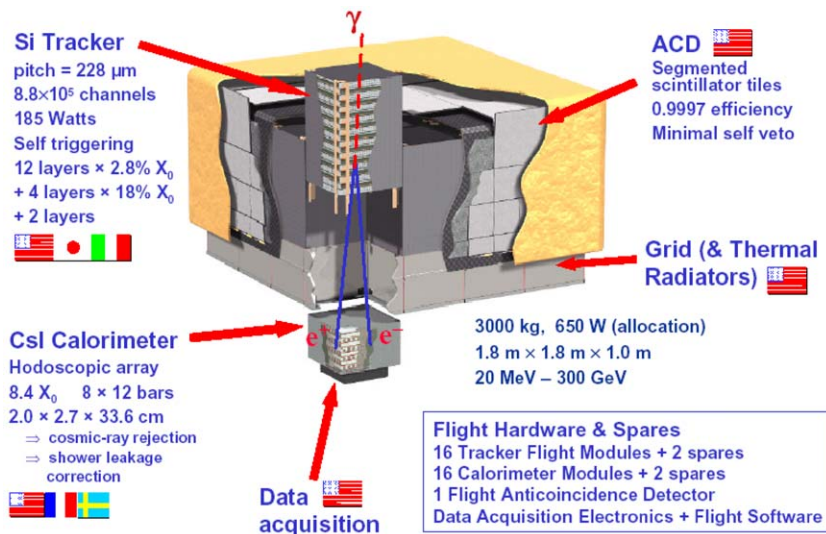


Fig. 7. General view of the Glast silicon-tracking system.

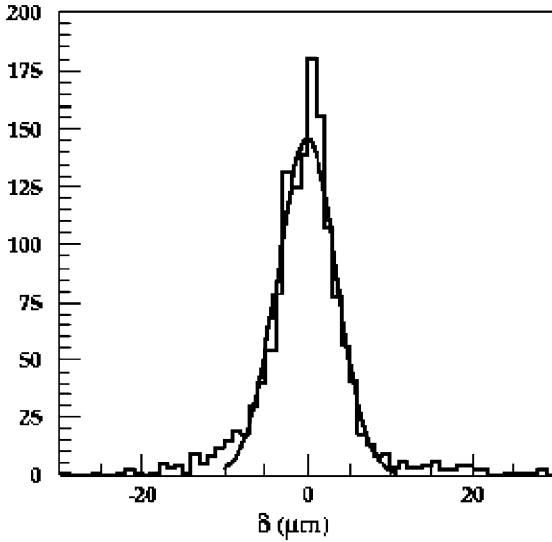


Fig. 8. Measured spatial resolution of the microstrip silicon detector of the Pamela experiment.

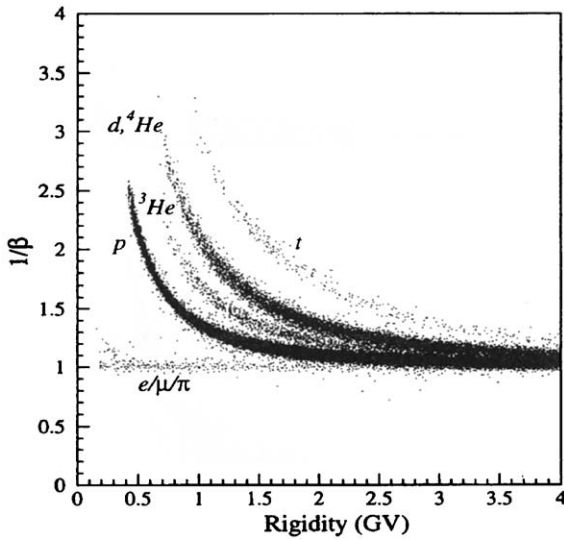


Fig. 9. Particle identification obtained by ToF measurements with BESS.

where  $R$  is the rigidity ( $\equiv p/Z$ ) and the atomic number  $Z$  is derived from

$$\frac{dE}{dx} \cong \left(\frac{Ze}{\beta}\right)^2 f(\beta).$$

Using scintillation counters with  $\sim 100$  ps time resolution, the Time Of Flight (TOF) method permits to separate e/p/He up to 2–3 GeV (see Fig. 9). However, the scintillator’s weight limits their dimensions (i.e., the detectors acceptance) and thickness (i.e. the time resolution

$$\sigma_{\text{TOF}} \propto \sqrt{n_{\text{ph}}},$$

where  $n_{\text{ph}}$  is the number of collected photons).

Furthermore, mechanical vibrations may affect the optical contact between a scintillator and its photodetector, which makes it necessary to use silicon rings (which are, however, subject to aging effects).

To extend or improve on the potential of the TOF method in particle identification, Cherenkov detectors may be used. Their threshold for light production is

$$\frac{p}{M} = \frac{1}{\sqrt{n^2 - 1}},$$

where  $p$  is the particle momentum,  $M$  is its mass and  $n$  the refractive index of the radiating material. Therefore, with a radiator such as aerogel ( $n=1.03$ ) a threshold at the  $\sim 4$  GeV/ $c$  level can be set for protons. The main problems

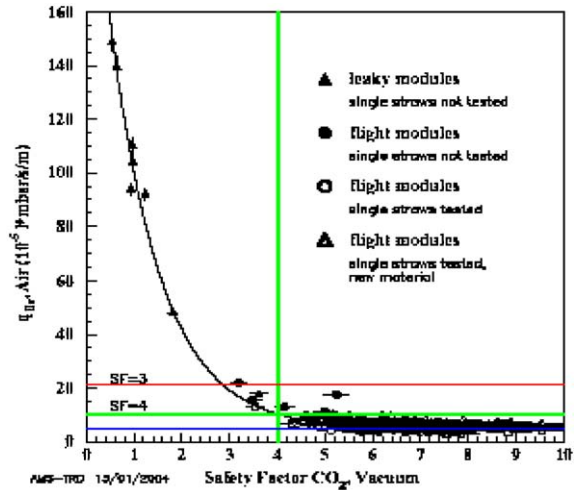


Fig. 10. Gas leakage measurements for straw tubes in the AMS-02 transition radiation detector. Tubes are selected so as to ensure an efficient operation over more than 12 years on the International Space Station (ISS).

for the use of Cherenkov detectors in space are the aging of the radiator and, if mirrors are needed such as for RICH detectors, the mechanical stability.

Above 1 GeV/c, Transition Radiation Detectors (TRD) can contribute at a  $10^{-2}$ – $10^{-3}$  level to discriminate  $p(\bar{p})$  from  $e^+(e^-)$ . The operation of TRDs in space is technologically challenging because of the presence of gas detectors (usually straw tubes). Furthermore, for optimally using the capabilities of a TRD, high thermal stability is needed because these devices suffer a 3–5% change in gain for each degree of temperature variation. When straw tubes are used to detect gamma rays, careful attention must be paid to gas leakage, which may reduce the lifetime of the device (see Fig. 10).

### 3.4. Energy measurements

Electromagnetic calorimeters with high granularity can reconstruct the longitudinal and transverse profile of the e.m. showers, thus providing e/p separation factors of the order of  $10^4$ , along with efficiencies greater than 90% for  $e^\pm$  detection. With imaging calorimeters it is also possible to measure energies up to  $\sim 1$  TeV even with a relatively small number of radiation lengths, provided the electronics has a sufficient dynamic range (from 1 up to  $\sim 10^5$  MIPs). In space the major limiting factor for the use of calorimeters is weight. When the acceptance ( $S$ ) and the number ( $n$ ) of radiation lengths ( $X_0$ ) are fixed, the weight  $W = \rho X_0(nS)$

Table 2  
Values of  $\rho X_0$  for different materials

	$\rho X_0$ (gr/cm <sup>2</sup> )	$X_0 \times \rho$		$\rho X_0$ (gr/cm <sup>2</sup> )	$X_0 \times \rho$
PbWO <sub>4</sub>	7.04	$0.85 \times 8.3$	Lead glass	14.3	$4.2 \times 3.4$
AMS (sampling ECAL)	6.9	$1.0 \times 6.9$	ThF <sub>4</sub>	7.45	$1.3 \times 6.3$
Pb(+ Si)	6.35	$0.56 \times 11.35$	PbF <sub>2</sub>	7.2	$0.93 \times 7.77$
BGO	7.91	$1.11 \times 7.13$	CaF <sub>3</sub> :Ce	6.1	$1.0 \times 6.1$
CsI	8.40	$1.86 \times 4.52$	NaI	9.5	$2.59 \times 3.67$

$\rho$  is the density in g/cm<sup>3</sup> and  $X_0$  is the radiation length in cm.

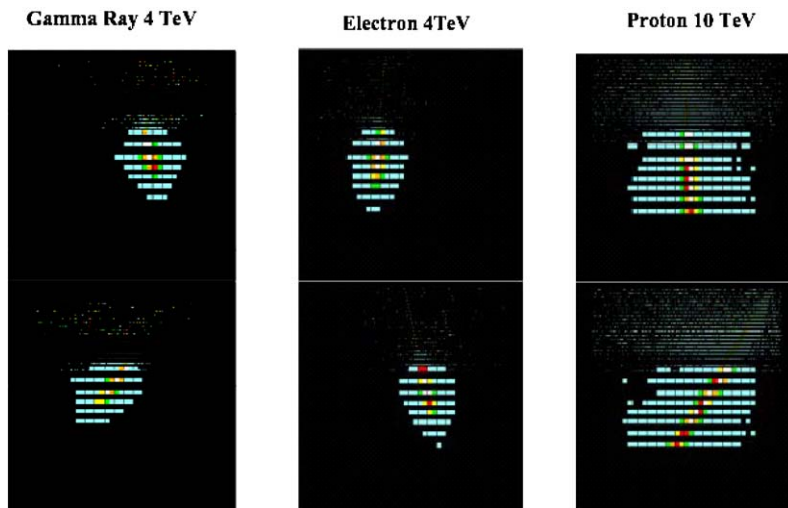


Fig. 11. Simulation of e.m. and hadronic cascades in the Calet experiment.



can be reduced by minimizing the quantity  $\rho X_0$ . In Table 2 the values of the quantity  $\rho X_0$  are reported for different materials commonly used for calorimeters.

Fig. 11 shows the structure of electromagnetic and hadronic cascades in the CALET imaging calorimeter (see [7]): the shower development is so different that a proton rejection power of  $10^5$ – $10^6$  is expected. High granularity calorimeters, like the one equipping the AMS-02 (see Fig. 12), permit also to reconstruct the incoming direction of  $\gamma$ 's with  $\sim 1^\circ$  of angular resolution (see Fig. 13).

In the EUSO experiment the particle energy is measured using a completely different approach (see Fig. 14): the observation of the Extended Air Shower (EAS) produced by primary particles interacting deep in the atmosphere. This method, requiring a large distance from the EAS and a large field of view, is complementary to the observation from the earth's surface: it covers a different energy range (even if partially overlapping) and suffers from different systematic effects. This experiment, in order to be suitable for space-based operation, is designed to have low mass, to be radiation hard and to guarantee stable and reliable operation.

### 3.5. Electronics and data acquisition systems

Electronics for experiments working in space must fulfill the following requirements:

- (a) low power dissipation

- (b) radiation hardness
- (c) stability over wide temperature range
- (d) mechanical stability
- (e) redundancy.

A generalized scheme for electronics is shown in Fig. 15. It is worth noting the number of DC–DC converters needed to provide the necessary voltages: they are crucial for saving power and weight. Redundancy is another mandatory requirement to ensure stable and reliable data taking over long periods of time.

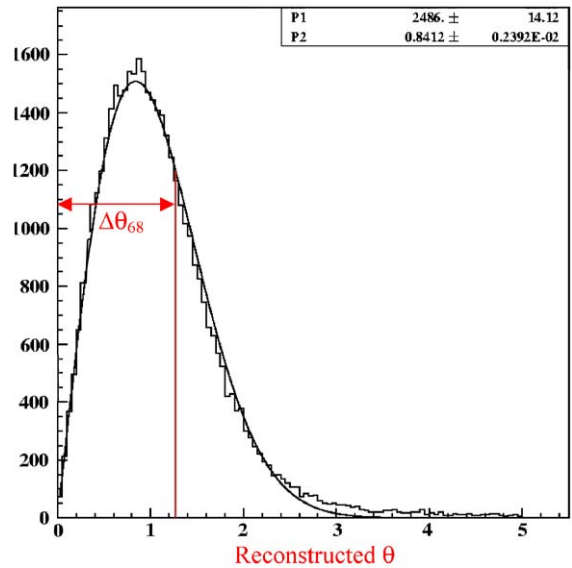


Fig. 13. Reconstructed angle for e.m. showers produced by electrons entering the AMS-02 calorimeter (ECAL) at  $0^\circ$ .

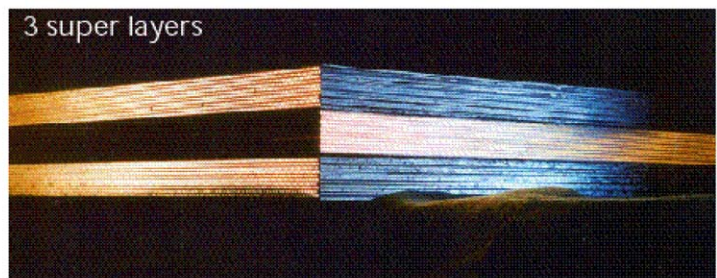
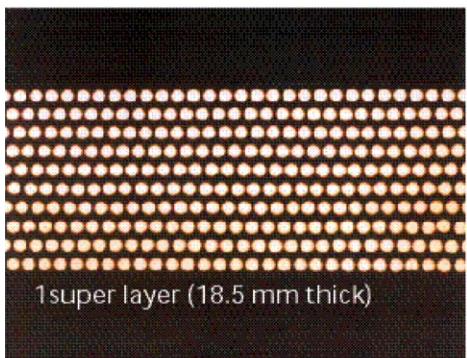


Fig. 12. The imaging calorimeter (ECAL) for AMS-02. This sampling calorimeter is made up of shaped lead foils and scintillating fibers.

Data acquisition systems operating in space perform conventional and “special” tasks:

(a) collection and packing of data

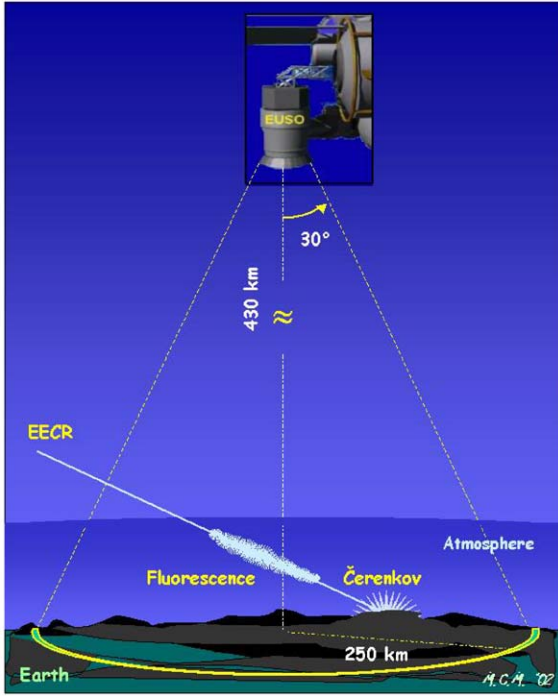


Fig. 14. The Euso approach to energy measurement. The CR energy is obtained from studying the Extended Air Shower.

- (b) temporary data storage before their transmission to Earth
- (c) reception, interpretation and execution of commands from Earth
- (d) registrations of problems and breakdowns
- (e) transmission of telemetry data (“house keeping”) to Earth
- (f) semi-automatic handling of electric power distribution
- (g) transmission of data according to agreed protocols.

In particular, temporary data storage is the only way to save registered events in case of data transmission problems.

#### 4. Conclusions

Experimentation in space calls for innovative solutions to original technological challenges. A simple comparison between the performance of Agile [8] and Egret [9] (see Table 3) demonstrates the impressive progress achieved over the last 20 years.

This success may convince us that high-energy experiments in space will provide a relevant contribution to new physics.

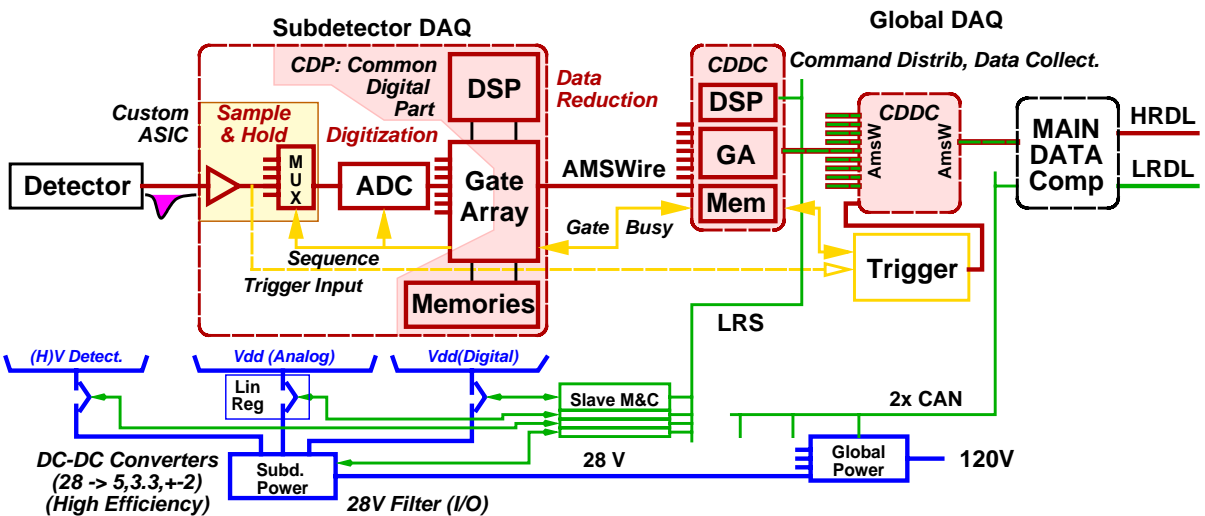


Fig. 15. Generalized scheme of electronics to be used in space.

Table 3  
A comparison between the Egret and Agile experiments

	AMS	BESS-polar
Field configuration	Dipole	Solenoid
Global magnetic dipole moment	No	Yes
Coil configuration	Race Track and Helmholtz	Single solenoid
Central field	0.87T	0.8T (~1T)
Peak field in coil	6.6T	1.1T
Bending power	0.78Tm <sup>2</sup>	0.45Tm <sup>2</sup>
Field variation in useful aperture	> 200%	< 10%
Current	459 A	389 A
Inductance	48.9 H	3.39 H
Stored energy	5100 kJ	260 kJ
Coil mass	2200 kg	< 43 kg
$E/M$ ratio	2.3 kJ/kg	6 kJ/kg
Cryogen	3000l	400l
Continuous operation	3 years	20 days
Features	No coil wall in aperture Dipole moment cancelled out	Low peak field Uniform Field

## References

- [1] O. Adriani, et al., Nucl. Instr. and Meth. A 511 (2003) 72.  
 [2] L. Latronico, Nucl. Instr. and Meth. A 511 (2003) 68.  
 [3] R. Battiston, Nucl. Phys. Proc. 113 (Suppl.) (2002) 9.  
 [4] EUSO, home page: <http://www.euso-mission.org>.  
 [5] R. Bellazzini, et al., The Glast Tracker Design Constr.  
 [6] A. Yamamoto, et al., Nucl. Phys. Proc. 113 (Suppl.) (2002) 208.  
 [7] Calet home page, <http://phwww.n.Kanagawa-u.ac.jp/calet/>.  
 [8] V. Cocco, et al., Nucl. Phys. Proc. 113 (Suppl.) (2002) 231.  
 [9] R. Mukherjee, et al., Astrophys J 490 (1997) 116.